Title

C60 Fullerols Enhance Copper Toxicity and Alter the Leaf Metabolite and Protein Profile in Cucumber

Journal

Environmental Science and Technology, 53(4)

ISSN

0013-936X

Authors

Zhao, Lijuan
Zhang, Huiling
Wang, Jingjing
et al.

Publication Date

2019-02-19

DOI

10.1021/acs.est.8b06758

Peer reviewed

Environmental Science & Technology

Article

Cite This: Environ. Sci. Technol. 2019, 53, 2171−2180

pubs.acs.org/est

C60 Fullerols Enhance Copper Toxicity and Alter the Leaf Metabolite and Protein Profile in Cucumber

Lijuan Zhao,[*,†] Huiling Zhang,[†] Jingjing Wang,[‡] Liyan Tian,[†] Fangfang Li,[‡] Sijin Liu,[§] Jose R. Peralta-Videa,[∥] Jorge L. Gardea-Torresdey,[∥] Jason C. White,[⊥] Yuxiong Huang,[#] Arturo Keller,[#] and Rong Ji[†]

[†]State Key Laboratory of Pollution Control and Resource Reuse, School of Environment, Nanjing University, Nanjing 210023, China

[‡]School of Materials Science and Engineering, Huazhong University of Science and Technology, 1037 Luoyu Road, Wuhan 430074, China

[§]State Key Laboratory of Environmental Chemistry and Ecotoxicology, Research Center for Eco-Environmental Sciences, Chinese Academy of Sciences, Beijing 100085, China

[∥]Chemistry Department, The University of Texas at El Paso, 500 West University Avenue, El Paso, Texas 79968, United States

[⊥]Department of Analytical Chemistry, The Connecticut Agricultural Experiment Station (CAES), New Haven, Connecticut 06504, United States

[#]Bren School of Environmental Science and Management, University of California, Santa Barbara, California 93106-5131, United States

Supporting Information

ABSTRACT: Abiotic and biotic stress induce the production of reactive oxygen species (ROS), which limit crop production. Little is known about ROS reduction through the application of exogenous scavengers. In this study, C60 fullerol, a free radical scavenger, was foliar applied to three-week-old cucumber plants (1 or 2 mg/plant) before exposure to copper ions (5 mg/plant). Results showed that C60 fullerols augmented Cu toxicity by increasing the influx of Cu ions into cells (170% and 511%, respectively, for 1 and 2 mg of C60 fullerols/plant). We further use metabolomics and proteomics to investigate the mechanism of plant response to C60 fullerols. Metabolomics revealed that C60 fullerols up-regulated antioxidant metabolites including 3-hydroxyflavone, 1,2,4-benzenetriol, and methyl *trans*-cinnamate, among others, while it down-regulated cell membrane metabolites (linolenic and palmitoleic acid). Proteomics analysis revealed that C60 fullerols up-regulated chloroplast proteins involved in water photolysis (PSII protein), light-harvesting (CAB), ATP production (ATP synthase), pigment fixation (Mg-PPIX), and electron transport (*Cyt b6f*). Chlorophyll fluorescence measurement showed that C60 fullerols significantly accelerated the electron transport rate in leaves (13.3% and 9.4%, respectively, for 1 and 2 mg C60 fullerols/plant). The global view of the metabolic pathway network suggests that C60 fullerols accelerated electron transport rate, which induced ROS overproduction in chloroplast thylakoids. Plant activated antioxidant and defense pathways to protect the cell from ROS damaging. The revealed benefit (enhance electron transport) and risk (alter membrane composition) suggest a cautious use of C60 fullerols for agricultural application.

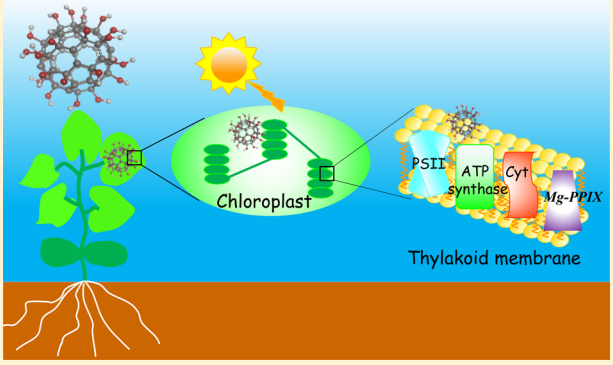

INTRODUCTION

By 2050, the global population is estimated to be nearly 9.6 billion, and as such, the global food demand is expected to increase by 70% to 100% to achieve food security.[1,2] Plants continuously face abiotic and biotic stresses during their life cycle,[3] which may prevent crops from reaching their full yield potential. Chemical and genetic approaches have been widely used to increase crop stress resistance. Nanotechnology-enabled solutions for improving stress resistance may offer new approaches to mitigate this issue.

In 2007, Yan et al. reported peroxidase-like activity of Fe_3O_4 nanoparticles (NPs).[4] Since then, nanomaterial-based enzyme

Received: December 3, 2018
Revised: January 14, 2019
Accepted: January 18, 2019
Published: January 18, 2019

DOI: 10.1021/acs.est.8b06758
Environ. Sci. Technol. 2019, 53, 2171−2180

mimetics have attracted more and more attention. A number of metal oxide NPs, such as CeO_2 and Mn_3O_4 NPs, have been found to have antioxidant enzyme-like function.[5,6] For example, CeO_2 NPs eliminate free radicals by mimicking the activities of superoxide dismutase, catalase, and peroxidase.[7−9] Wu et al. successfully alleviated declines in *Arabidopsis thaliana* (*L.*) *Heynh*. photosynthesis caused by abiotic stress by the application of CeO_2 NPs (50 mg L^{-1}).[10] More recently, the same group demonstrated that CeO_2 NPs are able to enhance leaf mesophyll K^+ retention, thereby improving *Arabidopsis* salinity tolerance.[11] This finding has triggered interest in exploring additional nanomaterials with unique physiochemical characteristics that may help plants tolerate or mitigate ROS to achieve full yield potential.

C60 fullerenes are closed hollow cages consisting of 60 three-coordinated carbon atoms. They are known as "radical sponges" exhibiting a powerful capacity for ROS scavenging due to delocalized double bonds on the surface of the molecule.[12] Fullerols C60(OH)n are water-soluble analogs of fullerene, which have a number of biomedical and pharmaceutical applications.[13] Similar to fullerene, the significant free radical scavenging capacities of fullerols have been reported.[14,15] Liu et al.[16] found that water-soluble fullerol is a highly efficient radical scavenger and proposed that this molecule could be an excellent candidate to stimulate plant defense in maize (*Zea mays* L.). Borisev et al.[17] reported that foliar application of fullerenol NPs alleviated drought induced oxidative stress in sugar beets (*Beta vulgaris* L.). However, contrary results were reported in another study, where fullerol amendment induced an overproduction of ROS.[18] Liu et al.[18] demonstrated that the adsorption of fullerene on plant cell walls led to overproduction of ROS, subsequently, disrupting both the cell wall and cell membranes. Therefore, to ensure the safe and sustainable use of C60 fullerols in agriculture,[17] it is important to understand the complex molecular mechanisms governing the interactions between C60 fullerols and crop species, simultaneously evaluating both benefits and risks.

High-throughput "omics" techniques are becoming powerful tools to detect holistic plant response to environmental stresses.[19] Metabolites are the downstream products of gene expression. Therefore, the changes in metabolic levels reflect the final response of an organism to environmental stress. Environmental metabolomics, in which small-molecule metabolites are identified and quantified simultaneously in an organism, provide a snapshot of what happened in the organism in response to a stressor.[20] Similarly, proteomics can accurately identify and quantify proteins involved in cellular events underlying stress response, including nanoparticle−plant interactions.[21−23] Multiomics approaches could provide a global and multilevel perspective on the plant stress responses.[24] However, multiomics analyses have been less used to study the interaction between nanoparticles and plants.

In our previous studies, Cu and $Cu(OH)_2$ NPs were found to induce oxidative stress via triggering the overgeneration of ROS.[25,26] Our hypothesis is that C60 fullerols with ROS scavenging capacities could help the plant to alleviate the oxidative stress. Here, hydrophilic and highly negatively charged C60 fullerols, with ROS scavenging capacities, were synthesized from C60 fullerene. The synthesized NPs were applied to living plants to evaluate their efficacy at alleviating Cu induced oxidative stress. Meanwhile, metabolomics and proteomic approaches were applied to understand the molecular mechanisms of the interaction between C60 fullerols and plants under Cu stress. The results provide valuable information for the possible application of fullerols in agriculture and for an evaluation of the environmental implications of this approach.

EXPERIMENTAL SECTION

Synthesis and Characterization of Water-Soluble C60 Derivatives. C60 fullerols, with 24−26 hydroxyl groups, were prepared by the reaction of fullerene with aqueous NaOH in the presence of tetrabutylammonium hydroxide (TBAH).[27] More details regarding the synthesis process are provided in the Supporting Information. The synthesized C60 fullerols were then characterized by Fourier transform infrared spectroscopy (FTIR; Bruker, Vertex 70, USA) and transmission electron microscopy (TEM; JEM-200CX, JEOL, Japan). The hydrodynamic diameter and zeta potential of the C60 fullerol suspension were determined by dynamic light scattering (DLS; Malvern, Nanosizer S90, USA).

ROS Scavenging Capacity of C60 Fullerols. The SOD-like activity of C60 fullerols were measured by a SOD assay kit with WST-1 (Nanjing Jiancheng Bioengineer, Nanjing, China). The catalase-like activity of C60 fullerols was determined based on a previously reported protocol with a slight modification.[28] The method to determine the hydroxyl radical scavenging capacity was adapted from Lu et al.[29] More details regarding the assay of ROS scavenging capacity of C60 fullerols are shown in the Supporting Information.

Plant Growth and Exposure Assay. Cucumber (*Cucumis sativus L.*) seeds (Zhongnong No.28 F1) were purchased from Hezhiyuan Seed Corporation (Shandong, China). One cucumber seed was sown in an individual 0.85 L plastic container (14 cm × 14 cm × 13 cm) containing 220 g of potting soil (0.68% N, 0.27% P_2O_5, and 0.36% K_2O, pH 4.28, Miracle-Gro, Beijing, China). The plants were grown in a greenhouse in a 6-h dark/18-h light regime. The temperature in the greenhouse were maintained at 28 °C during the day and 20 °C at night. The daily light integral was 180 $\mu mol \cdot m^{-2} \cdot s^{-1}$, and relative humidity was 60%. During the growth period, the plants were watered as needed, and no additional fertilizers were applied.

The foliar exposure was initiated when the cucumber seedlings were three-weeks-old. Six treatments were established, including (A) control (no C60 fullerols or Cu), (B) 1 mg C60 fullerols per plant, (C) 2 mg C60 fullerols per plant, (D) 5 mg Cu per plant, (E) 1 mg C60 fullerols + 5 mg Cu per plant, and (F) 2 mg C60 fullerols + 5 mg Cu per plant. For the treatments receiving both materials (group E and F), the C60 fullerols were applied 3 h prior to Cu application. The dose selection of Cu and C60 fullerols are based on preliminary experiments. Five replicate plants were grown for each treatment. The copper ion solution was prepared using $CuSO_4 \cdot 5H_2O$ (≥99.0%). Prior to spraying, the C60 fullerols suspension (100 and 200 mg L^{-1}) was sonicated (KH-100DB, Hechuang Utrasonic, Jiangsu, China) at 45 kHz for 30 min in Nanopure water to achieve a dispersed suspension. The foliar application was made two times per day in a 2-day exposure period using a hand-held spray bottle, with a total volume of 5 mL of copper ion suspension per plant and/or 10 mL of C60 fullerol suspension per plant, respectively. In this case, runoff into soil was not avoided.

Plasma Membrane Permeability Assay. Membrane integrity was estimated by measuring ion leakage from the leaf, following the method of Liu et al.,[30] with minor modifications. Specifically, 12 h after 2 days' foliar exposure, the leaf segments were cut and rinsed three times with Nanopure water to remove the ion leakage from the tissue during cutting.

DOI: 10.1021/acs.est.8b06758
Environ. Sci. Technol. 2019, 53, 2171−2180

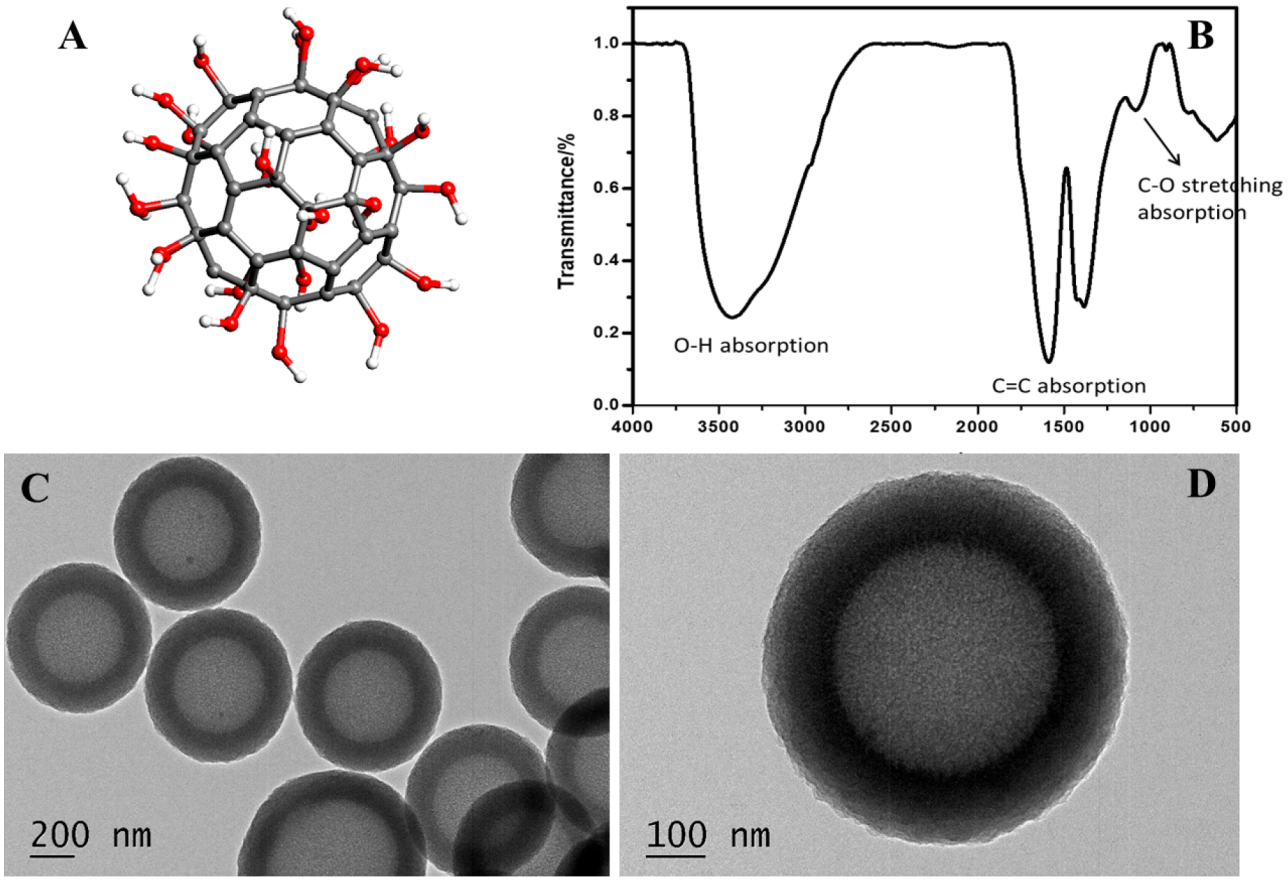

Figure 1. Characterization of the C60 fullerols. Molecular structure (A), IR spectra (B), and transmission electron microscope (TEM) micrographs of C60 fullerol aggregations, with a scale bar of 200 nm (C) and 100 nm (D), respectively.

The leaf segments were incubated in 50 mL vials containing 10 mL of Nanopure water for 3 h in a rotary shaker at 200 rpm at 25 °C (HZQ-F100, Taicang Huamei, China). After 3 h of incubation, the conductivity of the solution was measured (S_1) using a DDSJ-308A conductivity meter (INESA Scientific Instrument Ins., Shanghai, China). The solution was then boiled at 100 °C for 20 min. When the solution was cooled to room temperature (25 °C), the conductivity was measured again (S_2). The conductivity of Nanopure water was also determined (S_3). The relative membrane permeability (%) was calculated as $(S_1 - S_3)/(S_2 - S_3) \times 100\%$.

Lipid Peroxidation Analysis. Malondialdehyde (MDA) is the final product of fatty acid degradation and is indicative of lipid peroxidation. Here, MDA content was measured by the Thiobarbituric Acid Reactive Substances (TBARS) assay.[31] Briefly, 12 h after 2 days' foliar exposure, 0.2 g of fresh cucumber leaves were mixed with 4 mL of 0.1% trichloroacetic acid; the mixture was then centrifuged at 10 619*g* for 15 min. A 1 mL aliquot of the supernatant was mixed with 2 mL of 20% trichloroacetic acid and 2 mL of 0.5% thiobarbituric acid; then, the mixture was heated in a water bath at 95 °C for 30 min. After cooling, the UV absorbance was measured at 532 and 600 nm (UV-1800, Shimadzu Corporation, Kyoto, Japan). Lipid peroxidation was expressed as micromoles of MDA equivalent per gram of fresh weight leaf.

Inductively Coupled Plasma-Mass Spectrometry (ICP-MS) Analysis. Tissues for metal content analysis were oven-dried at 70 °C for 72 h and were then digested with plasma-pure HNO_3 and H_2O_2 (30%; 1:4) using a microwave digest system at 160 °C for 40 min (Milestone Ethos Up, Italy). For Cu and other macro- and micronutrients determination, the digested samples were analyzed by inductively coupled plasma-mass spectrometry (ICP-MS; NexION-300, PerkinElmer, USA).

GC-MS Based Leaf Metabolomics. Leaf metabolites were analyzed by gas chromatography−mass spectrometry (GC-MS). Briefly, an Agilent 7890B gas chromatograph coupled to an Agilent 5977A mass selective detector (Santa Clara, CA, USA), with a DB-5MS fused-silica capillary column (30 m × 0.25 mm internal diameter with 0.25 μm film; Agilent J & W Scientific, Folsom, CA, USA), was used to run the samples. Quantification was reported as peak height using a unique ion as the default. Metabolites were unambiguously assigned by the BinBase identifier numbers using retention index and mass spectrum as the two most important identification criteria. The data set of approached relative abundance of metabolites was processed for multivariate analysis. Both unsupervised principal component analysis (PCA) and supervised partial least-squares-discriminant analysis (PLS-DA) were performed using online resources (http://www.metaboanalyst.ca/).[32] More details regarding sample preparation and GC-MS analysis and multivariate analysis are shown in Supporting Information.

LC-MS/MS Based Leaf Proteomics. Leaf proteins were analyzed by LC-MS/MS. Briefly, the total protein collected from each leaf sample was digested with trypsin and then the peptides were labeled using a 4-plex iTRAQ reagent Multiplex kit (Applied Biosystems, Foster City, CA) according to the manufacturer's protocol. Data acquisition was performed with a Triple TOF 6600 mass spectrometer (SCIEX, Concord,

DOI: 10.1021/acs.est.8b06758
Environ. Sci. Technol. 2019, 53, 2171−2180

Ontario, Canada). The detailed methods regarding protein extraction and digestion, iTRAQ labeling, and LC-MS/MS analysis are provided in the Supporting Information.

Bioinformatics Analysis. The regulated proteins were defined as having a 1 fold change in abundance (Exposure Treatment/Control) more than 1.2 or less than 0.87 with a p value $\leq$0.05. GO annotations were retrieved from a large number of references, whereas KEGG70 and PPI analysis were performed using Omicsbean (http://www.omicsbean.cn).

Chlorophyll Fluorescence Measurements. The chlorophyll fluorescence parameters were measured using a portable miniaturized pulse-amplitude-modulated (MINI-PAM) chlorophyll fluorescence yield analyzer (Walz, Effeltrich, Germany). The maximum quantum yields of PSII [F_v/F_m], the effective quantum yields of PSII [$\Phi_{II} = (F_m' - F)/F_m'$], photochemical quenching (qP), nonphotochemical quenching (qN), and electron transport rate (ETR) were calculated based on the measured chlorophyll fluorescence.

RESULTS AND DISCUSSION

Synthesis and Characterization of C60 Fullerols. The structure of the fabricated C60 fullerols are shown in Figure 1A. As seen in Figure 1B, the FTIR spectra showed broad peaks at 1106, 1500, and 3421 cm^{-1}, which were attributed to the vibrations of C−O, C═C, and O−H bonds, respectively; this indicates that the fullerene was successfully surface modified with OH groups. The TEM images revealed that C60 fullerols formed homogenized core−shell nanostructures with an average diameter of approximately 500 nm (Figure 1C and D). Since the diameter of a single C60 fullerol molecule is about 1 nm, they easily aggregate under the force of hydrogen bonds in water. The DLS measured a hydrodynamic diameter of 100 and 200 mg L^{-1} of C60 fullerols at 389 ± 6 nm and 424 ± 74 nm, respectively; these values are similar to those obtained by TEM. In addition, the NPs were highly negatively charged, with zeta potentials of −39.5 ± 2.5 mV and −43.7 ± 7.2 mV for 100 and 200 mg L^{-1}, respectively. The highly negative charge of C60 fullerols has been attributed to bond stretching or deprotonation of the NPs hydroxyl groups due to the polarity of the water.[33]

ROS Scavenging Capacity of C60 Fullerols. Superoxide anion ($^{\bullet}O_2^-$), hydrogen peroxide (H_2O_2), and hydroxyl radical ($^{\bullet}OH$) are common ROS found in plants under abiotic and biotic stress. Table 1 shows that C60 fullerols reduced $^{\bullet}O_2^-$ in a dose-dependent manner, with a scavenging rate of 14 and 30% for 100 and 200 mg L^{-1} C60 fullerols, respectively. A possible mechanism of $^{\bullet}O_2^-$ scavenging by C60 derivatives has been proposed by Ali et al.[34] However, C60 fullerols had shown limited catalytic activity to scavenge H_2O_2 (1.7 and 2.7%), indicating weak CAT mimicking activity. In addition, the C60 fullerol NPs had a rapid and strong $^{\bullet}OH$ scavenging capacity, with 20% and 30% hydroxyl radical removal for 100 and 200 mg L^{-1} of C60 fullerols within 10 min. The observed $^{\bullet}O_2^-$ and $^{\bullet}OH$ scavenging capacities of C60 fullerols are consistent with previous reports.[21,35] Conversely, pristine C60 fullerene had relatively weak free radical scavenging capacity, compared to C60 fullerols (Table 1). Yin et al.[36] attribute the differences in free radical-scavenging capabilities to surface chemistry induced differences in electron affinity.

Table 1. ROS Scavenging Capacity of C60 Fullerols and Fullerene C60

	$^{\bullet}O_2^-$		H_2O_2		$^{\bullet}OH$	
	average (%)	SD	average (%)	SD	average (%)	SD
C60 fullerols (100 mg L^{-1})	14	0.65	1.7	1.1	20	0.62
C60 fullerols (200 mg L^{-1})	30	1.8	2.7	0.16	33	1.4
fullerene (100 mg L^{-1})	1.9	1.3	1.1	0.27	7.1	0.44
fullerene (200 mg L^{-1})	1.7	0.50	3.5	2.0	8.5	0.70

Performance of C60 Fullerols on Cu Induced Oxidative Stress. Copper was used as a model oxidative stress generator because Cu can catalyze the formation of ROS through Fenton and Haber−Weiss-type reactions.[37] Not surprisingly, 5 mg of Cu/plant treatment caused leaf chlorosis and senescence after 48 h of exposure (Figure 2I). Unexpectedly, C60 fullerols did not alleviate Cu induced toxicity in cucumber leaves. In fact, C60 fullerols tended to enhance the chlorosis symptoms visually (Figure 2I).

After 48 h of exposure, both C60 fullerol concentrations did not induce changes in MDA content, compared to the control (Figure 2 II), indicating that no lipid peroxidation occurred. Exposure to Cu resulted in a significant increase in MDA content (140%; $p \leq 0.05$) in leaves, compared to unexposed controls. However, pretreatment with C60 fullerols, at both concentrations, had no impact on the Cu induced MDA formation, reinforcing our phenotypic observations that C60 fullerols did not alleviate Cu induced oxidative stress in cucumber plants. On the contrary, plants pretreated with 1 and 2 mg/plant C60 fullerols appear to increase MDA content by 19% ($p = 0.09$) and 16% ($p = 0.06$), respectively, compared to plants exposed to only 5 mg Cu/plant.

To explain the mechanism behind the unexpected results, it was hypothesized that the C60 fullerols allowed an increased influx of Cu into leaves by changing either the membrane composition or cuticle permeability. To verify this hypothesis, ICP-MS was employed to determine the Cu content in cucumber tissues. Results showed that pretreatment with C60 fullerols significantly ($p \leq 0.05$) increased Cu accumulation in cucumber leaves in a dose-dependent manner (Figure 2 III). Lyon and Alvarez demonstrated that C60 fullerols could physically penetrate the lipid bilayer and disrupt the cell membrane integrity.[38] However, results showed that no cell membrane disruption occurred upon exposure to both doses of C60 fullerols (Figure 2IV). This suggests that C60 fullerols may possibly alter the membrane composition, instead of physically damaging it, to allow an increased influx of Cu. An alternative explanation for C60 fullerol-induced increase Cu uptake is the uptake of a fullerol−Cu complex, through the "Trojan horse effect."[39,40] But an additional experiment studying the C60 fullerol−Cu interaction is needed.

Metabolomics of Cucumber Leaves. An untargeted high-resolution GC-MS approach demonstrated substantial metabolic changes in cucumber leaves based on the data set of 351 identified and quantified metabolites. First, unsupervised PCA analysis was performed to generate an overview of the clustering information between the groups. The PCA score plot shows that Cu related groups (D, E, F) were clearly separated from non-Cu groups (A, B, C) along the first principle axis (PC1), which explained 25.4% of the total variability (Figure 3I). This indicates that copper markedly altered the metabolite profile in exposed cucumber plants, which is consistent with our previous study.[25] However, no noticeable separation between C60

DOI: 10.1021/acs.est.8b06758
Environ. Sci. Technol. 2019, 53, 2171−2180

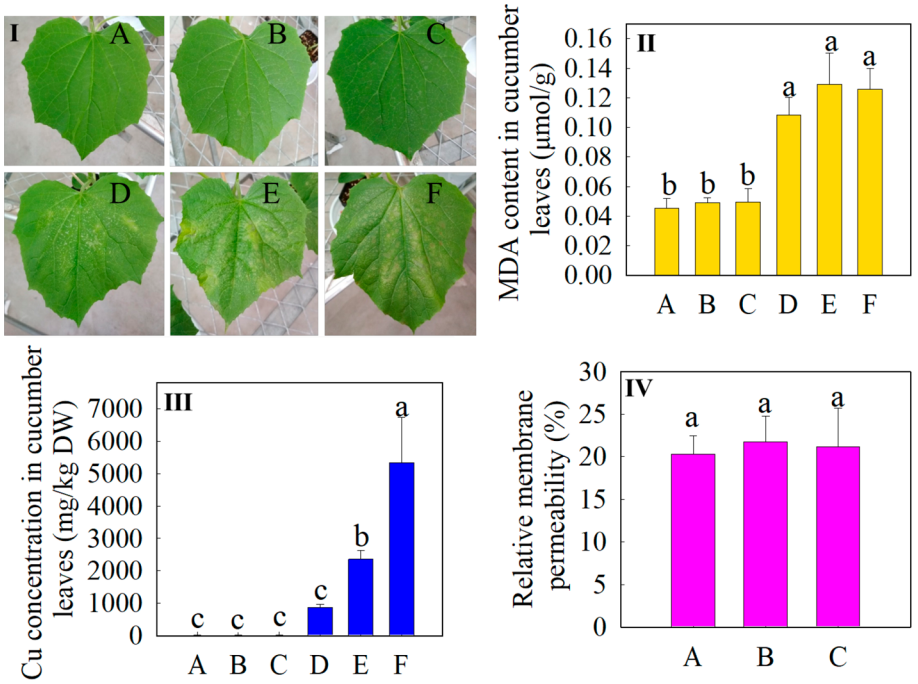

Figure 2. Impact of C60 fullerols on cucumber toxicity: Phenotypic images of cucumber leaf upon exposure to different doses of C60 fullerols and Cu (I); MDA content in cucumber leaves (II); biomass of cucumber plants (leaf + root) (III); Cu content in leaf tissues (IV). A–F represent different treatment groups: (A) control (neither C60 fullerols nor Cu); (B) 1 mg C60 fullerols/plant; (C) 2 mg C60 fullerols/plant; (D) 5 mg Cu/plant; (E) 1 mg C60 fullerols + 5 mg Cu/plant; (F) 2 mg C60 fullerols + 5 mg Cu/plant, respectively. Electrolyte leakage of cucumber leaf disc exposed to 1 and 2 mg of C60 fullerols NP/plant for 2 days (two times foliar application per day). Data are the average of three replicates. Error bars stand for standard deviation.

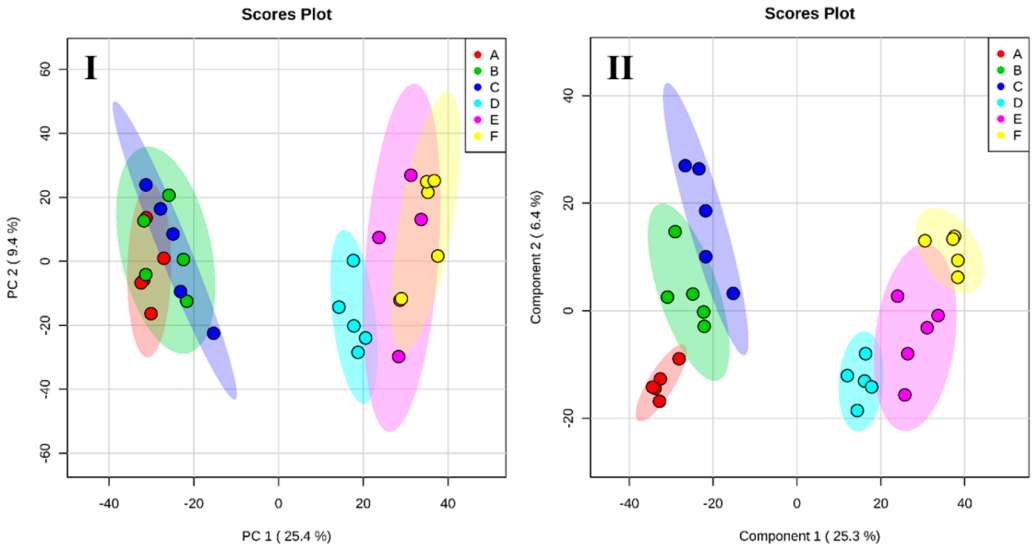

Figure 3. Principal component analysis (PCA) (A) and partial least-squares discriminate analysis (PLS-DA) (B) score plots of metabolic profiles in cucumber leaves treated with different dosage of C60 fullerols or Cu. The colored ellipses represent 95% confidence regions for each group. A–F represent different treatment groups: (A) control (neither C60 fullerols nor Cu); (B) 1 mg C60 fullerols/plant; (C) 2 mg C60 fullerols/plant; (D) 5 mg Cu/plant; (E) 1 mg C60 fullerols + 5 mg Cu/plant; (F) 2 mg C60 fullerols + 5 mg Cu/plant.

fullerols (group B and C) and the controls (group A) was observed in the PCA score plot. We further employed supervised PLS-DA analysis to maximize the separation between groups. The PLS-DA score plot (Figure 3II) shows that C60 fullerol groups (B and C) are generally separated from the control group (A) in a dose-dependent manner, along PC2, indicating that C60 fullerols, alone, altered the metabolite profile of cucumber leaves. Additionally, the presence of C60 fullerols (E and F) altered the Cu (D) induced metabolite profile in a dose-dependent fashion (Figure 3II), though the doses of C60 fullerols were much lower than that of Cu. The significantly changed metabolites were screened out by *t*-test as well, and results are present in a Venn diagram (Figure 4). Treatment of 1 mg C60 fullerols (B), 2 mg C60 fullerols (C), 5 mg Cu (D), 1 mg C60 fullerols + 5 mg Cu (E) and 2 mg C60 fullerols + 5 mg Cu (F) induced 20, 40, 117, 126, and 146 metabolite changes, respectively.

DOI: 10.1021/acs.est.8b06758
Environ. Sci. Technol. 2019, 53, 2171–2180

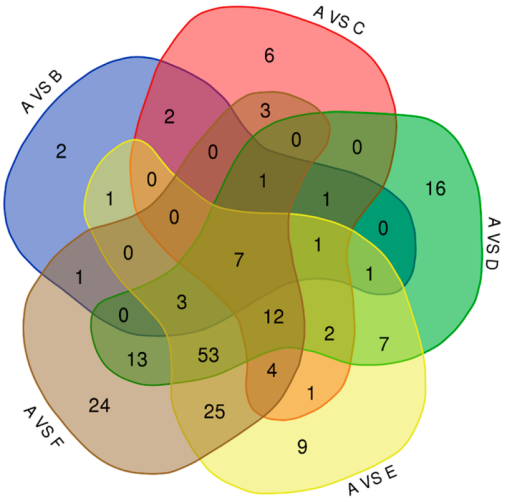

Figure 4. Venn diagram of significantly changed metabolites in cucumber leaves exposed to different dosage of C60 fullerols or Cu. A–F represent different treatment groups: (A) control (neither C60 fullerols nor Cu); (B) 1 mg C60 fullerols/plant; (C) 2 mg C60 fullerols/plant; (D) 5 mg Cu/plant; (E) 1 mg C60 fullerols + 5 mg Cu/plant; (F) 2 mg C60 fullerols + 5 mg Cu/plant.

Linolenic acid, a major component of the plasma membrane, was significantly decreased by C60 fullerols in a dose-dependent manner (Figure S1). The down-regulation of plasma membrane fatty acids is a strong indicator that cell membrane composition was altered by C60 fullerols. Yamauchi et al. demonstrated that chloroplasts are major organelles in which MDA is generated from peroxidized linolenic acid.[41] A previous study revealed that during stress or senescence, thylakoid membranes in chloroplasts are disintegrated and chlorophyll, and galactolipid are broken down. This, subsequently, results in the accumulation of toxic intermediates, such as tetrapyrroles, free phytol, and free fatty acids.[42] Additionally, phytol, a degradation product of chlorophyll, increased 37% and 74%, respectively, upon exposure to 1 and 2 mg/plant C60 fullerols (Figure S1). Moreover, several antioxidant related metabolites including 3-hydroxyflavone (backbone of all flavonols), 4-vinylphenol dimer, 1,2,4-benzenetriol, and quinic acid were up-regulated in response to C60 fullerols exposure (Figure S1). On the other hand, dehydroascorbic acid (DHA), an oxidized form of ascorbic acid (vitamin C, water-soluble antioxidant), was not detected in unexposed cucumber leaves but was significantly increased in plants exposed to C60 fullerols. Taken together, the fatty acids' down-regulation and antioxidant molecules' up-regulation may suggest that C60 fullerols triggered the excessive generation of ROS with an unknown mechanism, which is a quite interesting finding given that C60 fullerols are supposed to scavenge ROS as exogenous antioxidants.

Proteomics Analysis of Leaves. Isobaric tagging for relative and absolute quantitation (iTRAQ)-based proteomics unambiguously identified and quantified a total of 3125 proteins. Among them, 286 proteins were differentially expressed upon exposure, with 165 up-regulated and 121 down-regulated (fold change > 1.2 or < 0.87; $p \leq 0.05$) by C60 fullerols (Figure 5A). First, gene ontology (GO) analysis was used to gain insights into the biological processes, molecular functions, and cellular localization of the proteins differentially regulated by C60 fullerols. Changes in protein regulation induced by C60 fullerols were classified into 10 biological process categories, 10 cellular component categories, and 10 molecular function categories (Figure S2A). Proteins were also annotated according to the Kyoto Encyclopedia of Genes and Genomes (KEGG) pathway analysis. Results show that 10 pathways including photosynthesis, pyruvate metabolism, carbon metabolism, citrate cycle, carbon fixation, glyoxylate and dicarboxylate metabolism, glycolysis/gluconeogenesis, ribosome, porphyrin, and chlorophyll metabolism were significantly enriched (Figure S2B). The OmicsBean protein–protein interaction (PPI) network reveals that 16 proteins, with

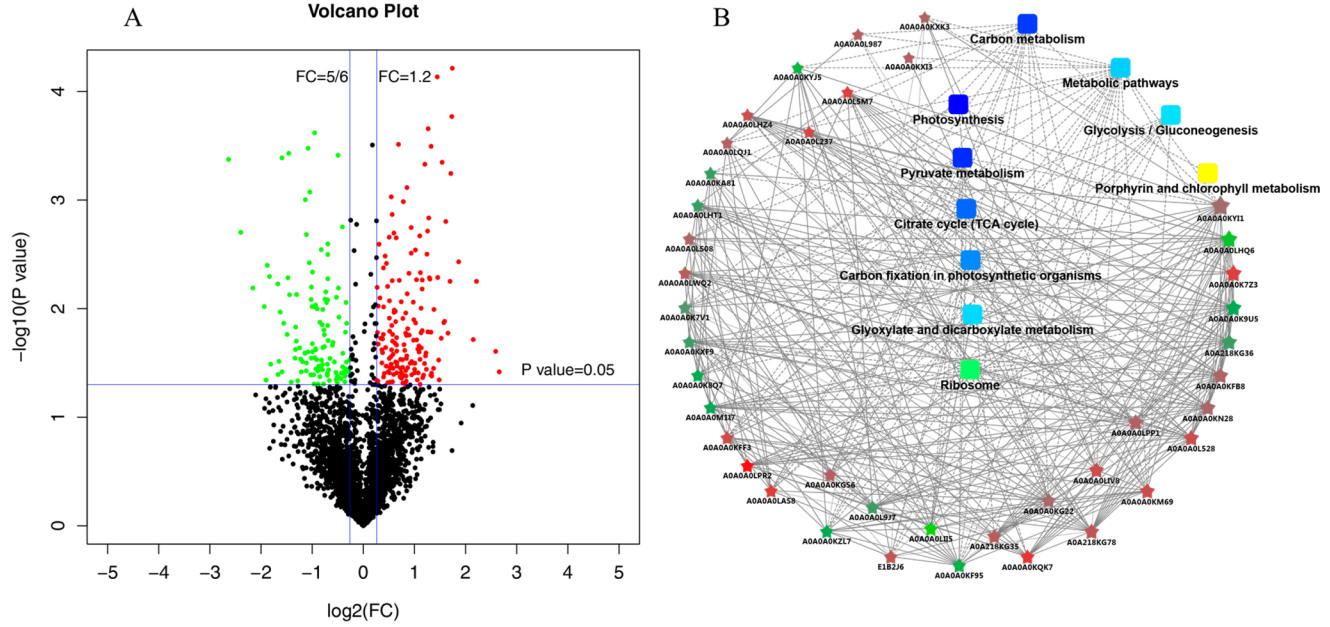

Figure 5. Quantitative proteomics data: (A) volcano plot of 286 differentially regulated ($p < 0.05$) proteins in cucumber leaves exposed to C60 fullerols. Red and green dots represent up-regulated (165) and down-regulated metabolites (121), respectively. (B) Protein–protein interaction networks of differentially expressed proteins.

DOI: 10.1021/acs.est.8b06758
Environ. Sci. Technol. 2019, 53, 2171–2180

five driver proteins, were centrally involved in energy metabolism (Figure 5 B). The differentially expressed proteins are related to photosynthesis and carbon fixation, energy, and defense, which will be further discussed.

Photosynthesis Related Proteins. Plants capture energy with their light-harvesting systems and chlorophylls, subsequently driving photosynthetic electron transport through the thylakoid membranes of the chloroplast.[43] The data showed that PSII proteins, which are related to water photolysis and electrons generation for all of photosynthesis to occur, were up-regulated (2.19-fold) by C60 fullerols exposure. In addition, cytochrome b6/f, which mediates electron transfer from photosystem II (PSII) to photosystem I (PSI), was found up-regulated (1.58-fold) by C60 fullerols exposure. In addition, the chloroplast ATP synthases use the proton motive force generated by photosynthetic electron transport to produce ATP from ADP.[44] Results showed that chloroplast ATP synthases increased 1.63-fold compared to the control. An exception is photosystem I (PSI) P700, which was decreased (0.52-fold) by C60 fullerol exposure. The function for this protein is to accept electrons from PSII and transfer NADP to NADPH. It is noteworthy that all the above-mentioned proteins are thylakoid membrane-localized proteins and participate in electron generation and transporting. The changes of these protein may indicate that C60 fullerols influence photosynthetic process.

Chlorophyll a/b binding proteins (CAB), light-harvesting complex (LHC) proteins, increased 1.4 and 2.7 fold, respectively, compared to control by C60 fullerols exposure. In addition, the abundance of Mg-protoporphyrin IX chelatase (Mg-PPIX, Mg-chelatase) was increased 1.46-fold by C60 fullerols. Mg-PPIX chelatase catalyzes the insertion of magnesium ions into protoporphyrin IX to yield Mg-protoporphyrin IX (Mg-PPIX), a chlorophyll precursor. Therefore, up-regulation of Mg-PPIX chelatase may indicate an effort to enhance chlorophyll biosynthesis. The cytochrome b559 β subunit (Cyt. *b*-559 β subunit), which plays a key role in photoprotection of photosystem II,[45] was also up-regulated 3.24-fold by C60 fullerols exposure. This suggests that cucumber leaves clearly responded to C60 fullerols exposure by upregulation of chlorophyll biosynthesis, promotion of the electron transport rate in photosystem II, and enhancement of light-harvesting.

The reason why C60 fullerols trigger the changes of thylakoid membrane-localized proteins is still unknown. C60 is a good acceptor of electrons, with the ability to accommodate up to six electrons reversibly. The capacities of C60 fullerols for electron acceptance may be attributed to changes in electron transport-related proteins. It is hypothesized that C60 fullerols accept the electrons from PSII. This triggers the up-regulation of electron transport-related proteins to compensate the electrons captured by C60 fullerols. However, further studies are needed to elucidate the underlying mechanism.

Chlorophyll fluorescence data verified that the electron transport rate (ETR) was significantly increased in leaves' exposure to both doses of C60 fullerols, from day 2 to day 5 (Figure 6A). The accelerated electron transport rate may explain the overproduced ROS, because the PS II and PS I located thylakoid membrane is the main site for ROS production. Additionally, the SPAD units (Figure 6B) and maximum quantum yield of PSII (F_v/F_m; Figure 6 C) of the cucumber leaf were unchanged by fullerol exposure. The effective quantum yield of PSII (ΦII) showed a significant difference between the

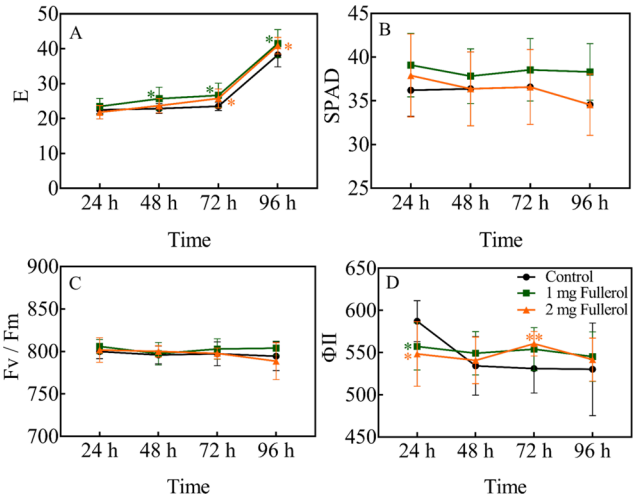

Figure 6. Chlorophyll fluorescence parameters. (A) Maximum PSII quantum yields (F_v/F_m). (B) Effective PSII quantum yields ($(F_m' - F)/F_m'$). (C) Electron transport rate (ETR). (D) Photochemical quenching (qP). (E) Nonphotochemical quenching (qN). (F) Relative chlorophyll content (SPAD) in cucumber leaves exposed to fullerols for 4 days. Data points represent the mean ± SD of n = 10 leaves for all treatments. Significance determined by Student's *t*-test; *P < 0.05, **P < 0.01.

control and fullerol treated plants at 24 and 72 h (Figure 6D). After first foliar application, ΦII was significantly decreased in leaves exposed to fullerols compared to the control. The tendency was kept on day 3, which means the high dose of C60 fullerol significantly increased the effective quantum yield.

Energy and Carbohydrate Metabolism. Proteins involved in energy and carbohydrate metabolism were divided into four groups: glycolysis, the pentose phosphate pathway, the TCA cycle, and others. Glycolysis is a metabolic pathway that oxidizes glucose to generate ATP, reductants, and pyruvate. It was found that the expression of enzymes catalyzing the steps of glycolysis, such as glucose-6-phosphate isomerase (GPI; 1.5-fold) and glyceraldehyde-3-phosphate dehydrogenase (GAPDH; 1.8-fold), were up-regulated by C60 fullerol exposure (Table 2). Alternatively, three proteins involved in the TCA cycle, including aconitate hydratase (Aconitase), succinate-CoA ligase (SCoAL), and malate dehydrogenase (MDH), were down-regulated (0.33−0.67) by C60 fullerol exposure (Table 2), suggesting inhibition of the TCA cycle. Glycolysis, the TCA cycle, and the mitochondrial electron transport chain are involved in plant respiration, which is a controlled oxidation of energy-rich photosynthetic end-products (i.e., starch and sucrose) to produce CO_2 and adenosine triphosphate (ATP).[46] The perturbation of energy related metabolism such as glycolysis and the TCA cycle may also be associated with excessive generation of ROS, as a previous report showed that oxidized lipids such as polyunsaturated fatty acid can inhibit TCA cycle activity.[47]

Protective, Detoxification, and Stress Responsive Proteins. The ITRAQ analysis indicated that the abundance of many proteins involved in detoxification and stress defense were up-regulated in cucumbers upon C60 fullerol exposure. Microsomal glutathione s-transferase (GST), and enzymes involved in protecting cell membranes from oxidative stress, was down-regulated by C60 fullerols, compared to the control. In addition, the expression of ferritin was up-regulated 2-fold. Ferritin is an iron-storage protein, which plays an important role

DOI: 10.1021/acs.est.8b06758
Environ. Sci. Technol. 2019, 53, 2171−2180

Table 2. Significantly Changed Proteins in Cucumber Leaf Exposed to 2 mg/Plant Fullerols

function	protein name	fold
photosynthesis	PSII proteins	2.19
	cytochrome b6/f mediates electron transfer	1.58
	chloroplast ATP synthases	1.63
	photosystem I (PSI) P700	0.52
	chlorophyll a/b binding proteins (CAB)	1.95
	Mg-protoporphyrin IX chelatase (Mg-PPIX, Mg-chelatase)	1.46
	cytochrome b559 β subunit	3.24
energy and carbohydrate metabolism	glucose-6-phosphate isomerase (GPI)	1.54
	glyceraldehyde-3-phosphate dehydrogenase (GAPDH)	1.78
	aconitate hydratase (aconitase)	0.66
	succinate-CoA ligase (SCoAL)	0.67
	malate dehydrogenase (MDH)	0.33
protective, detoxification, and stress responsive	microsomal glutathione s-transferase (GST)	0.59
	ferritin	2.03
	cysteine proteinase inhibitor (cystatins)	2.33
	tocopherol cyclase (TC)	2
	eptidyl-prolyl cis−trans isomerase (PPIases or immunophilins)	1.51
	HSP 70	1.47
	S-adenosylmethionine synthase (SAM)	1.57

in sequestering or releasing iron upon demand.[48] In addition to buffering iron, previous studies have also revealed that plant ferritins protect cells against oxidative damage by scavenging ROS.[49] The cysteine proteinase inhibitor (cystatins) increased 2-fold, which has the potential to improve resistance against pathogens that possess cysteine proteinases.[50]

Tocopherol cyclase (TC), which is related to tocopherol content and oxidative stress,[51] was up-regulated by C60 fullerol exposure. Tocopherol is a strong antioxidant, which is crucial for scavenging ROS during oxidative stress.[52] TC is synthesized in the inner envelope of chloroplasts and accumulates in all chloroplast membranes, where it provides protection against oxidative degradation. Phytol, a precursor of tocopherol biosynthesis, increased concurrently with TC, which indicates C60 fullerol induced oxidative stress and activated the antioxidant defense system.

In addition to the above antioxidant and detoxification related proteins, Peptidyl-prolyl cis−trans isomerase (PPIases or immunophilins), which is involved in plant defense and disease response,[53] was up-regulated by C60 fullerol exposure. Apart from antioxidants, HSP 70, which helps to refold misfolded proteins, was also found to be up-regulated. S-adenosylmethionine synthase (SAM), a precursor of ethylene and polyamines, was up-regulated by 1.56-fold. This indicates that C60 fullerols not only enhance the photosynthesis but also activate the defense system, which is consistent with the metabolic results.

Linking the metabolomics and proteomics data, a hypothesis is proposed that the accelerated electron transport induced by C60 fullerols in reaction centers of photosystem I (PSI) and photosystem II (PS II) triggered the overproduction of ROS. Plants up-regulated antioxidant molecules and defense related proteins to protect the thylakoid from damage. The excessive generation of ROS also caused perturbation in carbon metabolism.

Environmental Implications. In this study, a carbon-based nanomaterial, C60 fullerol, was used as exogenous antioxidant to alleviate Cu-induced oxidative stress in cucumber plants. Unexpectedly, C60 fullerol enhanced Cu induced toxicity in cucumber plants, by enhancing the influx of Cu into the cells.

Scheme 1. Summary Scheme Showing the Main Changes Induced by C60 Fullerol in Cucumber Leaves, Detected at the Metabolite and Protein Levels[a]

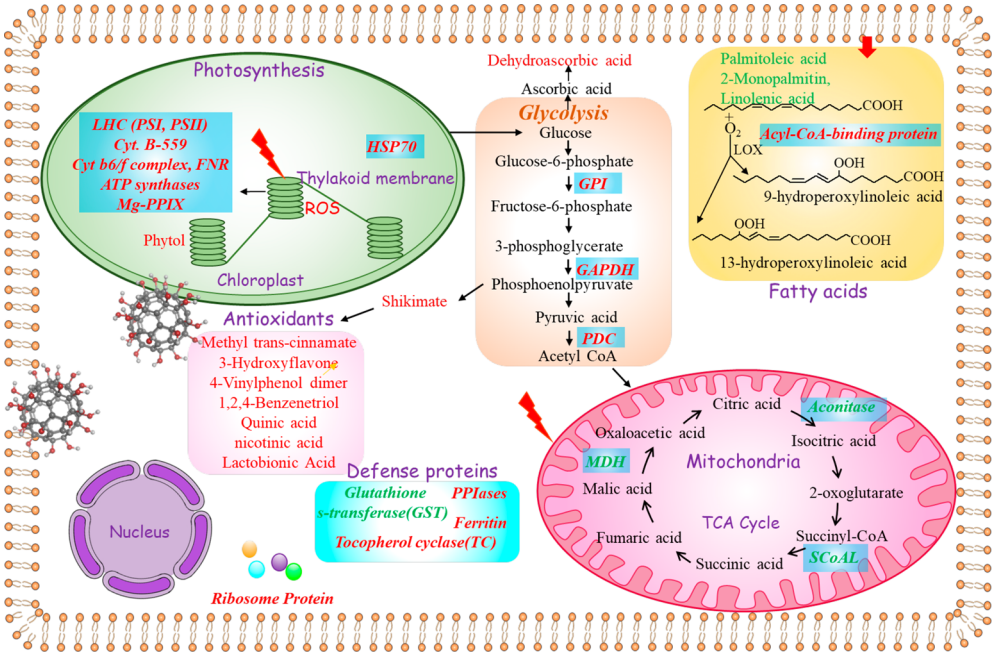

[a]Statistically differentially regulated metabolites and proteins are displayed in italics, with up-regulation in red and down-regulation in green.

DOI: 10.1021/acs.est.8b06758
Environ. Sci. Technol. 2019, 53, 2171−2180

Although no visual toxicity symptoms were observed, metabolomics reveals that C60 fullerol induced metabolic network reprogramming in leaves, including down-regulation of fatty acids and up-regulation of low molecular weight antioxidant compounds (Scheme 1), which indicates membrane composition alteration and stress response. Proteomics analysis revealed that C60 fullerol up-regulated chloroplast membrane proteins involved in water photolysis, electron transport, light-harvesting, and pigment fixation. Additionally, C60 fullerols disturbed energy related pathways, including up-regulation of glycolysis related proteins and down-regulation of TCA cycle related proteins (Scheme 1). A chlorophyll fluorescence experiment verified that C60 fullerols are able to enhance the electron transport rate in the cucumber leaf. A thorough understanding of the underlying mechanism behind the molecular changes imposed by C60 fullerol may enable their future safe and sustainable use in agriculture.

■ ASSOCIATED CONTENT

Supporting Information

The Supporting Information is available free of charge on the ACS Publications website at DOI: 10.1021/acs.est.8b06758.

The significantly changed metabolites in cucumber leaves exposed to C60 fullerols (Figure S1); bioinformatic analysis of proteomics data (Figure S2); the selected setting for Database Searching (Table S1) (PDF)

■ AUTHOR INFORMATION

Corresponding Author

*Tel.: +86 025-8968 0581. Fax: +86 025-8968 x0581. E-mail: ljzhao@nju.edu.cn.

ORCID

Lijuan Zhao: 0000-0002-8481-0435
Fangfang Li: 0000-0001-6850-2857
Sijin Liu: 0000-0002-5643-0734
Jorge L. Gardea-Torresdey: 0000-0002-9467-0536
Jason C. White: 0000-0001-5001-8143
Yuxiong Huang: 0000-0001-8124-643X
Arturo Keller: 0000-0002-7638-662X
Rong Ji: 0000-0002-1724-5253

Notes

The authors declare no competing financial interest.

■ ACKNOWLEDGMENTS

This work was funded by the National Key Research and Development Program of China under 2016YFD0800207 and National Natural Science Foundation of China under 21876081 and 21661132004. Any opinions, finding, and conclusions or recommendations expressed in this material are those of the authors and do not necessarily reflect the views of National Science Foundation of China.

■ REFERENCES

(1) Rodrigues, S. M.; Demokritou, P.; Dokoozlian, N.; Hendren, C. O.; Karn, B.; Mauter, M. S.; Sadik, O. A.; Safarpour, M.; Unrine, J. M.; Viers, J.; Welle, P.; White, J. C.; Wiesner, M. R.; Lowry, G. V. Nanotechnology for sustainable food production: promising opportunities and scientific challenges. *Environ. Sci.: Nano* **2017**, *4* (4), 767−781.

(2) Mueller, N. D.; Gerber, J. S.; Johnston, M.; Ray, D. K.; Ramankutty, N.; Foley, J. A. Closing yield gaps through nutrient and water management. *Nature* **2012**, *490*, 254.

(3) Ranty, B.; Aldon, D.; Cotelle, V.; Galaud, J.-P.; Thuleau, P.; Mazars, C. Calcium Sensors as Key Hubs in Plant Responses to Biotic and Abiotic Stresses. *Front. Plant Sci.* **2016**, *7*, 327.

(4) Gao, L.; Zhuang, J.; Nie, L.; Zhang, J.; Zhang, Y.; Gu, N.; Wang, T.; Feng, J.; Yang, D.; Perrett, S.; Yan, X. Intrinsic peroxidase-like activity of ferromagnetic nanoparticles. *Nat. Nanotechnol.* **2007**, *2*, 577.

(5) Yao, J.; Cheng, Y.; Zhou, M.; Zhao, S.; Lin, S.; Wang, X.; Wu, J.; Li, S.; Wei, H. ROS scavenging Mn3O4 nanozymes for in vivo anti-inflammation. *Chemical Science* **2018**, *9* (11), 2927−2933.

(6) Lee, S. S.; Song, W.; Cho, M.; Puppala, H. L.; Nguyen, P.; Zhu, H.; Segatori, L.; Colvin, V. L. Antioxidant Properties of Cerium Oxide Nanocrystals as a Function of Nanocrystal Diameter and Surface Coating. *ACS Nano* **2013**, *7* (11), 9693−9703.

(7) Bhushan, B.; Gopinath, P. Antioxidant nanozyme: a facile synthesis and evaluation of the reactive oxygen species scavenging potential of nanoceria encapsulated albumin nanoparticles. *J. Mater. Chem. B* **2015**, *3* (24), 4843−4852.

(8) Pirmohamed, T.; Dowding, J. M.; Singh, S.; Wasserman, B.; Heckert, E.; Karakoti, A. S.; King, J. E. S.; Seal, S.; Self, W. T. Nanoceria exhibit redox state-dependent catalase mimetic activity. *Chem. Commun.* **2010**, *46* (16), 2736−2738.

(9) Tian, Z.; Li, J.; Zhang, Z.; Gao, W.; Zhou, X.; Qu, Y. Highly sensitive and robust peroxidase-like activity of porous nanorods of ceria and their application for breast cancer detection. *Biomaterials* **2015**, *59*, 116−124.

(10) Wu, H.; Tito, N.; Giraldo, J. P. Anionic Cerium Oxide Nanoparticles Protect Plant Photosynthesis from Abiotic Stress by Scavenging Reactive Oxygen Species. *ACS Nano* **2017**, *11* (11), 11283−11297.

(11) Wu, H.; Shabala, L.; Shabala, S.; Giraldo, J. P. Hydroxyl radical scavenging by cerium oxide nanoparticles improves Arabidopsis salinity tolerance by enhancing leaf mesophyll potassium retention. *Environ. Sci.: Nano* **2018**, *5* (7), 1567−1583.

(12) Injac, R.; Prijatelj, M.; Strukelj, B. Fullerenol Nanoparticles: Toxicity and Antioxidant Activity. In *Oxidative Stress and Nanotechnology: Methods and Protocols*; Armstrong, D., Bharali, D. J., Eds.; Humana Press: Totowa, NJ, 2013; pp 75−100.

(13) Rokitskaya, T. I.; Antonenko, Y. N. Fullerenol C60(OH)24 increases ion permeability of lipid membranes in a pH-dependent manner. *Biochim. Biophys. Acta, Biomembr.* **2016**, *1858* (6), 1165−1174.

(14) Hao, T.; Li, J.; Yao, F.; Dong, D.; Wang, Y.; Yang, B.; Wang, C. Injectable fullerenol/alginate hydrogel for suppression of oxidative stress damage in brown adipose-derived stem cells and cardiac repair. *ACS Nano* **2017**, *11* (6), 5474−5488.

(15) Yui, N.; Yoshioka, H.; Fujiya, H.; Musha, H.; Karasawa, R.; Yudoh, K. Water-soluble C60-(OH)24 fullerene hydroxide as a therapeutic agent against the degeneration of articular cartilage in osteoarthritis. *Osteoarthritis and Cartilage* **2015**, *23*, A164−A165.

(16) Liu, F.-y.; Xiong, F.-x.; Fan, Y.-k.; Li, J.; Wang, H.-z.; Xing, G.-m.; Yan, F.-m.; Tai, F.-j.; He, R. Facile and scalable fabrication engineering of fullerenol nanoparticles by improved alkaline-oxidation approach and its antioxidant potential in maize. *J. Nanopart. Res.* **2016**, *18* (11), 338.

(17) Borišev, M.; Borišev, I.; Župunski, M.; Arsenov, D.; Pajević, S.; Ćurčić, Ž.; Vasin, J.; Djordjevic, A. Drought Impact Is Alleviated in Sugar Beets (Beta vulgaris L.) by Foliar Application of Fullerenol Nanoparticles. *PLoS One* **2016**, *11* (11), e0166248−e0166248.

(18) Liu, Q.; Zhang, X.; Zhao, Y.; Lin, J.; Shu, C.; Wang, C.; Fang, X. Fullerene-Induced Increase of Glycosyl Residue on Living Plant Cell Wall. *Environ. Sci. Technol.* **2013**, *47* (13), 7490−7498.

(19) Michaletti, A.; Naghavi, M. R.; Toorchi, M.; Zolla, L.; Rinalducci, S. Metabolomics and proteomics reveal drought-stress responses of leaf tissues from spring-wheat. *Sci. Rep.* **2018**, *8* (1), 5710.

(20) Guijas, C.; Montenegro-Burke, J. R.; Warth, B.; Spilker, M. E.; Siuzdak, G. Metabolomics activity screening for identifying metabolites that modulate phenotype. *Nat. Biotechnol.* **2018**, *36* (4), 316.

(21) Majumdar, S.; Almeida, I. C.; Arigi, E. A.; Choi, H.; VerBerkmoes, N. C.; Trujillo-Reyes, J.; Flores-Margez, J. P.; White, J.

DOI: 10.1021/acs.est.8b06758
Environ. Sci. Technol. 2019, 53, 2171−2180

C.; Peralta-Videa, J. R.; Gardea-Torresdey, J. L. Environmental Effects of Nanoceria on Seed Production of Common Bean (Phaseolus vulgaris): A Proteomic Analysis. *Environ. Sci. Technol.* **2015**, *49* (22), 13283−13293.
(22) Verano-Braga, T.; Miethling-Graff, R.; Wojdyla, K.; Rogowska-Wrzesinska, A.; Brewer, J. R.; Erdmann, H.; Kjeldsen, F. Insights into the Cellular Response Triggered by Silver Nanoparticles Using Quantitative Proteomics. *ACS Nano* **2014**, *8* (3), 2161−2175.
(23) Bramini, M.; Sacchetti, S.; Armirotti, A.; Rocchi, A.; Vázquez, E.; León Castellanos, V.; Bandiera, T.; Cesca, F.; Benfenati, F. Graphene Oxide Nanosheets Disrupt Lipid Composition, Ca2+ Homeostasis, and Synaptic Transmission in Primary Cortical Neurons. *ACS Nano* **2016**, *10* (7), 7154−7171.
(24) Fukushima, A.; Kanaya, S.; Nishida, K. Integrated network analysis and effective tools in plant systems biology. *Front. Plant Sci.* **2014**, *5*, 598−598.
(25) Zhao, L.; Huang, Y.; Paglia, K.; Vaniya, A.; Wancewicz, B.; Keller, A. A. Metabolomics Reveals the Molecular Mechanisms of Copper Induced Cucumber Leaf (Cucumis sativus) Senescence. *Environ. Sci. Technol.* **2018**, *52* (12), 7092−7100.
(26) Zhang, H.; Du, W.; Peralta-Videa, J. R.; Gardea-Torresdey, J. L.; White, J. C.; Keller, A.; Guo, H.; Ji, R.; Zhao, L. Metabolomics Reveals How Cucumber (Cucumis sativus) Reprograms Metabolites To Cope with Silver Ions and Silver Nanoparticle-Induced Oxidative Stress. *Environ. Sci. Technol.* **2018**, *52* (14), 8016−8026.
(27) Li, J.; Takeuchi, A.; Ozawa, M.; Li, X.; Saigo, K.; Kitazawa, K. C60 fullerol formation catalysed by quaternary ammonium hydroxides. *J. Chem. Soc., Chem. Commun.* **1993**, No. 23, 1784−1785.
(28) Wang, Y.-J.; Dong, H.; Lyu, G.-M.; Zhang, H.-Y.; Ke, J.; Kang, L.-Q.; Teng, J.-L.; Sun, L.-D.; Si, R.; Zhang, J.; Liu, Y.-J.; Zhang, Y.-W.; Huang, Y.-H.; Yan, C.-H. Engineering the defect state and reducibility of ceria based nanoparticles for improved anti-oxidation performance. *Nanoscale* **2015**, *7* (33), 13981−13990.
(29) Lu, M.; Zhang, Y.; Wang, Y.; Jiang, M.; Yao, X. Insight into Several Factors that Affect the Conversion between Antioxidant and Oxidant Activities of Nanoceria. *ACS Appl. Mater. Interfaces* **2016**, *8* (36), 23580−23590.
(30) Liu, J. J.; Wei, Z.; Li, J. H. Effects of copper on leaf membrane structure and root activity of maize seedling. *Bot. Stud.* **2014**, *55* (1), 47.
(31) Jambunathan, N. Determination and Detection of Reactive Oxygen Species (ROS), Lipid Peroxidation, and Electrolyte Leakage in Plants. In *Plant Stress Tolerance: Methods and Protocols*; Sunkar, R., Ed.; Humana Press: Totowa, NJ, 2010; pp 291−297.
(32) Xia, J.; Sinelnikov, I. V.; Han, B.; Wishart, D. S. MetaboAnalyst 3.0−making metabolomics more meaningful. *Nucleic Acids Res.* **2015**, *43* (W1), W251−W257.
(33) Ratnikova, T. A.; Bebber, M. J.; Huang, G.; Larcom, L. L.; Ke, P. C. Cytoprotective properties of a fullerene derivative against copper. *Nanotechnology* **2011**, *22* (40), 405101.
(34) Ali, S. S.; Hardt, J. I.; Quick, K. L.; Sook Kim-Han, J.; Erlanger, B. F.; Huang, T.-t.; Epstein, C. J.; Dugan, L. L. A biologically effective fullerene (C60) derivative with superoxide dismutase mimetic properties. *Free Radical Biol. Med.* **2004**, *37* (8), 1191−1202.
(35) Osuna, S.; Swart, M.; Solà, M. On the Mechanism of Action of Fullerene Derivatives in Superoxide Dismutation. *Chem. - Eur. J.* **2010**, *16* (10), 3207−3214.
(36) Yin, J.-J.; Lao, F.; Fu, P. P.; Wamer, W. G.; Zhao, Y.; Wang, P. C.; Qiu, Y.; Sun, B.; Xing, G.; Dong, J.; Liang, X.-J.; Chen, C. The scavenging of reactive oxygen species and the potential for cell protection by functionalized fullerene materials. *Biomaterials* **2009**, *30* (4), 611−621.
(37) Vanacker, S. A. B. E.; Tromp, M. N. J. L.; Haenen, G. R. M. M.; Vandervijgh, W. J. F.; Bast, A. Flavonoids as Scavengers of Nitric Oxide Radical. *Biochem. Biophys. Res. Commun.* **1995**, *214* (3), 755−759.
(38) Lyon, D. Y.; Alvarez, P. J. J. Fullerene Water Suspension (nC60) Exerts Antibacterial Effects via ROS-Independent Protein Oxidation. *Environ. Sci. Technol.* **2008**, *42* (21), 8127−8132.
(39) Wang, Z.; Xia, T.; Liu, S. Mechanisms of nanosilver-induced toxicological effects: more attention should be paid to its sublethal effects. *Nanoscale* **2015**, *7* (17), 7470−7481.
(40) Deng, R.; Lin, D.; Zhu, L.; Majumdar, S.; White, J. C.; Gardea-Torresdey, J. L.; Xing, B. Nanoparticle interactions with co-existing contaminants: joint toxicity, bioaccumulation and risk. *Nanotoxicology* **2017**, *11* (5), 591−612.
(41) Yamauchi, Y.; Furutera, A.; Seki, K.; Toyoda, Y.; Tanaka, K.; Sugimoto, Y. Malondialdehyde generated from peroxidized linolenic acid causes protein modification in heat-stressed plants. *Plant Physiol. Biochem.* **2008**, *46* (8), 786−793.
(42) Lippold, F.; vom Dorp, K.; Abraham, M.; Hölzl, G.; Wewer, V.; Yilmaz, J. L.; Lager, I.; Montandon, C.; Besagni, C.; Kessler, F.; Stymne, S.; Dörmann, P. Fatty Acid Phytyl Ester Synthesis in Chloroplasts of Arabidopsis Arabidopsis. *Plant Cell* **2012**, *24* (5), 2001−2014.
(43) Yamori, W.; Takahashi, S.; Makino, A.; Price, G. D.; Badger, M. R.; von Caemmerer, S. The roles of ATP synthase and the cytochrome b6/f complexes in limiting chloroplast electron transport and determining photosynthetic capacity. *Plant Physiol.* **2011**, *155*, 956.
(44) Zhang, L.; Duan, Z.; Zhang, J.; Peng, L. BIOGENESIS FACTOR REQUIRED FOR ATP SYNTHASE 3 facilitates assembly of the chloroplast ATP synthase complex in Arabidopsis. *Plant Physiol.* **2016**, pp.00248.2016.
(45) Chu, H.-A.; Chiu, Y.-F. The Roles of Cytochrome b 559 in Assembly and Photoprotection of Photosystem II Revealed by Site-Directed Mutagenesis Studies. *Front. Plant Sci.* **2016**, *6*, 1261−1261.
(46) O'Leary, B.; Plaxton, W. Plant Respiration. *eLS*; John Wiley & Sons, Ltd.: Chichester, UK, **2016**; pp 1−11.
(47) Ito, J.; Taylor, N.; Castleden, I.; Weckwerth, W.; Millar, A. L.; Heazlewood, J. A Survey of the Arabidopsis thaliana Mitochondrial Phosphoproteome. *Proteomics* **2009**, *9*, 4229−4240, DOI: 10.1002/pmic.200900064.
(48) Briat, J. F. Roles of ferritin in plants. *J. Plant Nutr.* **1996**, *19* (8−9), 1331−1342.
(49) Ravet, K.; Touraine, B.; Boucherez, J.; Briat, J.-F.; Gaymard, F.; Cellier, F. Ferritins control interaction between iron homeostasis and oxidative stress in Arabidopsis. *Plant J.* **2009**, *57* (3), 400−412.
(50) Masoud, S. A.; Johnson, L. B.; White, F. F.; Reeck, G. R. Expression of a cysteine proteinase inhibitor (oryzacystatin-I) in transgenic tobacco plants. *Plant Mol. Biol.* **1993**, *21* (4), 655−663.
(51) Kanwischer, M.; Porfirova, S.; Bergmüller, E.; Dörmann, P. Alterations in tocopherol cyclase activity in transgenic and mutant plants of Arabidopsis affect tocopherol content, tocopherol composition, and oxidative stress. *Plant Physiol.* **2005**, *137* (2), 713−723.
(52) Munné-Bosch, S.; Alegre, L. The function of tocopherols and tocotrienols in plants. *Crit. Rev. Plant Sci.* **2002**, *21* (1), 31−57.
(53) Mokryakova, M. V.; Pogorelko, G. V.; Bruskin, S. A.; Piruzian, E. S.; Abdeeva, I. A. The role of peptidyl-prolyl cis/trans isomerase genes of Arabidopsis thaliana in plant defense during the course of Xanthomonas campestris infection. *Russ. J. Genet.* **2014**, *50* (2), 140−148.

DOI: 10.1021/acs.est.8b06758
Environ. Sci. Technol. 2019, 53, 2171−2180